Interface Focus

Interface Focus (2011) **1**, 48–60
doi:10.1098/rsfs.2010.0012
Published online 1 December 2010

Skin surface temperature rhythms as potential circadian biomarkers for personalized chronotherapeutics in cancer patients

Christopher G. Scully[1,2], Abdoulaye Karaboué[3,4], Wei-Min Liu[1], Joseph Meyer[1], Pasquale F. Innominato[3,4,5], Ki H. Chon[2], Alexander M. Gorbach[1] and Francis Lévi[3,4,5,*]

[1]*Biomedical Engineering and Physical Science, National Institute of Biomedical Imaging and Bioengineering, National Institutes of Health, Bethesda, MD, USA*
[2]*Department of Biomedical Engineering, Worcester Polytechnic Institute, Worcester, MA, USA*
[3]*INSERM, UMRS776, Rythmes Biologiques et Cancers, Villejuif 94807, France*
[4]*Université Paris-Sud, UMR-S0776, Orsay 91405, France*
[5]*Assistance Publique-Hôpitaux de Paris, Unité de Chronothérapie, Département de Cancérologie, Hôpital Paul Brousse, Villejuif 94807, France*

Chronotherapeutics involve the administration of treatments according to circadian rhythms. Circadian timing of anti-cancer medications has been shown to improve treatment tolerability up to fivefold and double efficacy in experimental and clinical studies. However, the physiological and the molecular components of the circadian timing system (CTS), as well as gender, critically affect the success of a standardized chronotherapeutic schedule. In addition, a wrongly timed therapy or an excessive drug dose disrupts the CTS. Therefore, a non-invasive approach to accurately detect and monitor circadian rhythms is needed for a dynamic assessment of the CTS in order to personalize chronomodulated drug delivery schedule in cancer patients. Since core body temperature is a robust circadian biomarker, we recorded temperature at multiple locations on the skin of the upper chest and back of controls and cancer patients continuously. Variability in the circadian phase existed among patch locations in individual subjects over the course of 2–6 days, demonstrating the need to monitor multiple skin temperature locations to determine the precise circadian phase. Additionally, we observed that locations identified by infrared imaging as relatively *cool* had the largest 24 h temperature variations. Disruptions in skin temperature rhythms during treatment were found, pointing to the need to continually assess circadian timing and personalize chronotherapeutic schedules.

Keywords: chronotherapeutics; circadian rhythm; biomarker; body temperature; cancer; personalized medicine

1. INTRODUCTION

Circadian rhythms (with approximately a 24 h period) have been shown for most biological variables in many living organisms, including cyanobacteria, plants, flies, rodents and humans [1,2]. Rhythms on other time scales also characterize biological functions, such as ultradian hourly rhythms in pituitary hormonal secretions or NF-κB cellular signalling pathways, and yearly rhythms in the reproductive behaviour of mammals [3–6]. Circadian rhythms are especially relevant for anti-cancer therapy, since they regulate drug metabolism and gate cell division over the 24 h [5,7]. Circadian rhythms are generated within each cell by molecular clocks, consisting of interwoven transcription/translation feedback loops involving 15 'clock' genes [4]. The molecular clocks are coordinated during the 24 h by an array of physiological rhythms, which are generated by the suprachiasmatic nuclei (SCN). This circadian pacemaker, located in the hypothalamus, receives daily inputs from environmental cycles, and generates rhythmic physiological outputs, such as rest–activity, body temperature and hormonal secretions [5]. The circadian timing system (CTS) assembles these different components and regulates bodily functions over the 24 h. As a result, the CTS

*Author for correspondence (francis.levi@inserm.fr).

One contribution of 16 to a Theme Issue 'Advancing systems medicine and therapeutics through biosimulation'.

Received 25 October 2010
Accepted 4 November 2010

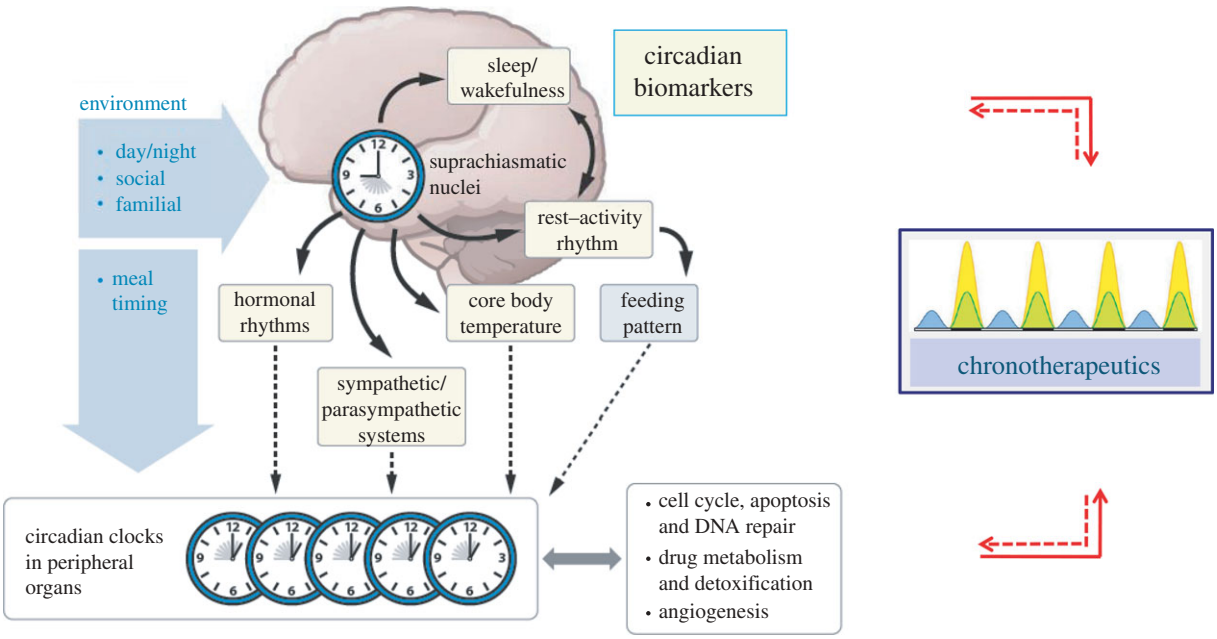

Figure 1. Schematic of the circadian timing system (CTS). The CTS is composed of a hypothalamic pacemaker, the suprachiasmatic nuclei SCN, an array of SCN-generated circadian physiology outputs, and molecular clocks in the cells of peripheral tissues. Molecular clocks rhythmically control xenobiotic metabolism and detoxification, cell cycle, apoptosis, DNA repair and angiogenesis over a 24 h period. The CTS is synchronized with time cues provided by light–dark cycles and other environmental factors. Circadian physiology outputs can also serve as CTS biomarkers. Chronotherapeutics aim at improving chemotherapy tolerability and efficacy through the adjustment of drug delivery to the CTS, which can in turn be influenced by the treatment regimen (Reproduced with permission from *Annu. Rev. Pharmacol. Toxicol.* **50**. Copyright © 2010 by Annual Reviews; http://www.annualreviews.org).

determines optimal times of day or night when anti-cancer medications are best tolerated and most effective. Cancer chronotherapeutics integrate the CTS control of biological functions into the design of chronomodulated drug delivery patterns in order to enhance tolerability and/or efficacy (figure 1; [5]).

In mice or rats with similarly synchronized CTS, the tolerability of 40 anti-cancer drugs varied two- to several fold as a function of circadian timing [5]. Moreover, anti-tumour efficacy was usually largest following treatment near the time of best tolerability, as shown for 28 anti-cancer medications [5]. Mathematical models have pinpointed several differences between the biological dynamics in healthy tissues and those in cancer, which could account for this coincidence between chronotolerance and chronoefficacy. These include a differential in (i) circadian entrainment, which is effective in healthy cells, but often lacking in cancer cells, (ii) cell cycle phase variability, (iii) cell cycle length, and (iv) tumour cell growth rate [8–11].

Clinical trials have shown the relevance of chronomodulated infusions of chemotherapy in cancer patients. Results from preclinical and clinical studies determined a standardized chronomodulated delivery pattern for the anti-cancer drugs 5-fluorouracil–leucovorin (5-FU–LV) and oxaliplatin, with peak flow rates at 4.00 h for 5-FU–LV and at 16.00 h for oxaliplatin (chronoFLO) [5]. Such a chronotherapeutic schedule standardized for the entire patient population improved tolerability up to fivefold and nearly doubled anti-tumour efficacy as compared with both constant rate infusion and chronomodulated schedules with peak times of drug delivery shifted by 9–12 h [7,12]. In a subsequent randomized trial, chronoFLO prolonged survival in men, but not in women suffering from metastatic colorectal cancer, as compared with conventional treatment delivery [13]. This finding has just been confirmed in the first meta-analysis of three randomized trials involving 842 patients with metastatic colorectal cancer [14]. Moreover, while optimal circadian timing remained within a 6 h window in men, a larger inter-patient variability in optimal timing was apparent in women, demonstrating that a standardized chronomodulated delivery schedule may not be appropriate for an entire patient population [7]. In addition, severe toxicities were encountered 25–50% more frequently in women as compared with men, irrespective of scheduling [7,13]. These findings led us to hypothesize that excessive toxicity from chemotherapy suppresses the circadian mechanisms needed for chronotherapeutic optimization, and that this occurs more frequently in women than in men.

Indeed, circadian disruption resulted from wrongly timed or excessively dosed chemotherapy, as shown for 12 anti-cancer agents in experimental models [5]. Furthermore, circadian disruption accelerated cancer growth in experimental models, as well as in cancer patients [15–20]. Experimental studies provided consistent evidence that the reinforcement of the CTS through small molecules, such as seliciclib, or meal timing inhibited cancer growth [21,22]. Thus, circadian biomarkers are needed for tailoring cancer chronotherapeutics to the dynamics of circadian organization of an individual patient in order to personalize the drug delivery schedules.

Appropriate circadian biomarkers should help identify the optimal endogenous timing of anti-cancer treatments in an individual patient, detect CTS alterations and guide adequate treatment adjustments. CTS disruption through ablation of the hypothalamic pacemaker, iterative alterations of the light–dark cycles, clock gene mutations or cancer chemotherapy result in rest–activity rhythm alterations, so that this rhythm has played a major role for circadian phenotyping [4]. Rest–activity rhythm has been monitored non-invasively using a wrist actigraph in large cohorts of cancer patients. Statistically significant relations were found between rest–activity rhythm parameters and patient symptoms and quality of life [18]. Most importantly, rest–activity parameters also displayed statistically significant and independent prognostic values for patient survival [19,23]. However, the square waveform of the rest–activity pattern makes it a poor biomarker for the circadian phase since it mostly provides information on start and termination times of rest and activity spans, with their respective variability in amount of activity.

Core body temperature is a circadian biomarker that appears to robustly reflect CTS pacemaker function and provide relevant information on phase and amplitude both in experimental models [5] and in humans [24–26]. Furthermore, the circadian rhythm in body temperature plays an important role in the coordination of molecular clocks, as well as clock-controlled pathways in experimental tumours [22,27]. Based on this knowledge, we hypothesize that temperature monitoring may be an appropriate biomarker for personalization of cancer chronotherapeutics. On the one hand, core body temperature cannot be easily monitored non-invasively or continuously in patients. On the other hand, skin temperature patterns can display variable links with core body temperature and sleep patterns according to site of measurement, levels of activity of the subject and environmental conditions [28,29]. In addition, there is typical heterogeneity in skin temperature within a given area, possibly in relation to different properties in temperature regulation, and the underlying microvasculature. We approached these problems through placing thermal sensing patches over locally warmer or cooler skin surface areas as identified with an infrared (IR) camera, in the upper thorax and back torso of each subject. In this pilot study, we provide the first analysis of skin temperature dynamics recorded at multiple sites in healthy individuals and in cancer patients undergoing cancer chronotherapy. We further show inter- and intra-individual circadian dynamics which support the future aim of using temperature as a biomarker to personalize chronotherapeutics.

2. SUBJECTS AND METHODS

2.1. Subjects and experimental design

The study involved five controls, three women and two men, aged 26–61 years, and four cancer patients, three men and one woman, aged 27–69 years. All subjects signed informed consent that explained the study, its goals, procedures and possible drawbacks and expectations. Two of the control subjects had intercurrent minor health events, which were unrelated to the study and required medication intake. Three cancer patients had received extensive chemotherapy and iterative surgical procedures for metastatic colorectal cancer. Two of them were receiving chronomodulated chemotherapy during the study with irinotecan, 5-fluorouracil, leucovorin and oxaliplatin over 4 consecutive days (chronoIFLO4) combined with bevacizumab for one patient, and cetuximab for the other one [30,31]. One patient with metastatic renal cell carcinoma was taking a single daily oral dose of everolimus in the late evening and gliclazide in the morning, following prior failure of sunitinib (table 1). The five controls and two cancer patients underwent their ordinary daily activities during monitoring, which was not the case for the two hospitalized cancer patients receiving intensive chronotherapy. All subjects kept a precise diary of their daily activities, including times of awakening and retiring, meal times, times of bath or shower, times of going in or out and times and doses of medication intake.

2.1.1. Thermal measurements. Wireless skin surface temperature patches (Philips Respironics, MA, USA), with set sampling rates of 15 s, temperature resolution of 0.01°C and battery life of 240 h were placed on each subject's skin to monitor temperature continuously for 39–120 h. Each subject carried a VitalSense monitor (Philips Respironics) that was capable of monitoring up to 10 patches simultaneously, and the subjects were asked to keep the monitor within the 2 m reception range at all times.

Six or seven skin surface temperature patches were placed on the chest and upper back of each subject, according to IR imaging with an FLIR SC7700 camera (FLIR Systems ATS, France) with 0.015°C temperature resolution in the 3–5 μm wavelength (at 640 × 512 pixels per image). The warmest and coolest locations of both the chest and the upper back of each subject were marked with a surgical pen, and the thermal sensor of each patch was positioned directly at the mark (figure 2). Images were acquired before and immediately after patch placement as well as before and immediately after patch removal. Table 2 summarizes the patch placement and recording characteristics for healthy controls (HC) and patients (PAT).

All subjects also carried an iButton temperature sensor (Maxim Integrated Products, Inc., CA, USA) and were instructed to keep the sensor within 2 m of their body; this monitored ambient air temperature with a sampling rate of 1/60 to 1/600 s, set according to the duration of a subject's participation in the study.

2.1.2. Rest–activity measurements. The rest–activity pattern was monitored in all the subjects using a Mini-Motionlogger wristwatch accelerometer (Ambulatory Monitoring Inc., NY, USA). Activity data were recorded simultaneously using zero-crossing mode (ZCM) and proportional integrating measure (PIM) algorithms. ZCM counts the number of times within a set epoch (1 min) that the accelerometer changes

Table 1. Subject characteristics.

	sex	age (years)	height (cm)	weight (kg)	start date	end date	intercurrent diseases	ongoing treatment (s)	comment
HC 1	F	26	165	65	07 Mar 2010	09 Mar 2010	infectious (chronic) sinusitis, menses on second day	montélukast (Singulair) 10 mg d^{-1} at 20 h, desloratadine (Aerius) 5 mg d^{-1} at 20 h	—
HC 2	M	61	182	93	07 Mar 2010	10 Mar 2010	none	none	—
HC 3	F	51	162	60	09 Mar 2010	11 Mar 2010	fracture of the fifth metatarsus of the left foot in consolidation	sodic fondaparinux (Arixtra) 2.5 mg d^{-1} (subcutaneous) at 22.30 h	—
HC 4	F	35	157	59	11 Mar 2010	14 Mar 2010	none	none	—
HC 5	M	26	180	75	23 Mar 2010	28 Mar 2010	none	none	—
PAT 1	M	69	160	55	16 Mar 2010	18 Mar 2010	multiple metastases from colon cancer (liver, lung and lymph nodes)	none	last course of AVIFF[a] (16–20 Mar 2010)
PAT 2	M	55	178	67	16 Mar 2010	18 Mar 2010	multiple liver metastases from colon cancer	Erb + chronoFLO[b]	daily supportive medications
PAT 3	F	27	162	59	17 Mar 2010	22 Mar 2010	multiple liver, lung and bone metastases from colon cancer	Erb + chronoIFLO4[c]	daily supportive medications
PAT 4	M	68	170	82	22 Mar 2010	25 Mar 2010	brain, lung, adrenal, skin, pancreatic and lymph node metastases from renal cancer	everolimus (Afinitor) 10 mg at 23.00 h in the evening, gliclazide (Diamicron) 80 mg at 09.00 h in the morning	stereotaxic radiotherapy on frontal and occipital metastases on 24 Feb 2010

[a]Bevazucimab (1 day infusion) + chronomodulated irinotecan-5-fluorouracil-folinic acid (3 days, infusion).
[b]Cetuximab (1 day infusion) + chronomodulated 5-fluorouracil, folinic acid and oxaliplatin (3 days, infusion).
[c]Cetuximab (1 day infusion) + chronomodulated irinotecan, 5-fluorouracil, folinic acid and oxaliplatin (3 days, infusion).

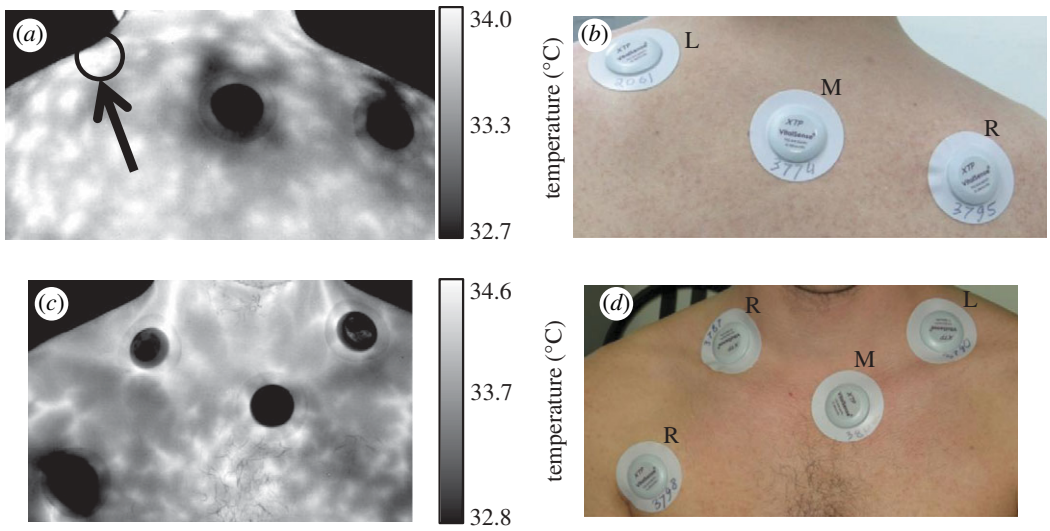

Figure 2. Example of patch placement on a control subject. Placement of patches was guided using infrared (IR) imaging to identify relatively warm and cool locations. Three patches were placed on the back of this subject, shown by the (*a*) infrared image and (*b*) visible image. In the visible image (*b*), superimposed 'R', 'M' and 'L' signify right, middle and left, respectively, and numbers on the patches represent a unique identification number for each patch. Lighter colours in the infrared images represent warmer temperatures. A warm location on the skin before patch placement is identified in (*a*) by the arrow and circle surrounding the region where the patch will be placed. (*c*) Infrared and (*d*) visible images of the subject's chest show four patches that are already placed, two on the right, one in the middle and one on the left side of the chest.

Table 2. Skin surface patch placement information. Number of patches analysed out of the total number of patches placed was determined based on the criteria in the text. Patches were placed on the chest or upper back, right, middle or left and on relatively warm or cool locations of the torso, as described in the text.

subject	recording length (h)	analysed–placed	chest–back	right–middle–left	warm–cool
HC 1	46.7	6–6	3–3	4–0–2	4–2
HC 2	39.3	1–6	3–3	4–0–2	4–2
HC 3	46.8	6–6	3–3	2–2–2	4–2
HC 4	72.3	4–5	3–2	2–1–2	3–2
HC 5	110.3	7–7	4–3	3–2–2	5–2
PAT 1	49.3	5–6	3–3	3–1–2	4–2
PAT 2	74.6	2–5	2–3	1–1–3	3–2
PAT 3	120.1	4–6	3–3	2–1–3	4–2
PAT 4	77.1	6–6	3–3	2–2–2	4–2

direction and is valid for studying rest–activity patterns. PIM counts the total amount of motion by the wristwatch accelerometer during the epoch, and was used in this study to look at relationships between skin temperature and activity, because it is a more specific indicator of motion intensity than ZCM [32,33].

2.2. Data analyses

All data analysis was performed using Matlab R2010b (The Mathworks, MA, USA), according to subject group (healthy controls versus patients), IR characterization of skin temperature (warm versus cool) and thermal patch placement (chest versus back; right versus middle versus left). All temperature time series with less than 20 per cent data loss were retained and were subjected to a cubic spline procedure to interpolate lost data points (table 2).

2.2.1. Wavelet analysis to identify temperature rhythm spectra. Time–frequency spectra were generated using continuous wavelet analysis to obtain increased time resolution at the frequencies of interest in the ultradian and circadian domains, with respective periods of 1–18 h and 18.01–30 h. The gapped wavelet transform (GWT) was used for time–frequency analysis, because it is not limited by a cone of influence that shortens the usable data length at low frequencies, as is the standard continuous wavelet transform [34–36]. A Morlet wavelet with $\omega_0 = 6$ was used as the mother wavelet. Each skin temperature dataset was low-pass filtered with a cut-off frequency of 0.0083 Hz and downsampled to 0.0167 Hz prior to GWT computation. GWT was computed with a frequency range of $0.0081–8.97 \times 10^{-6}$ Hz (period range of 0.03–30 h).

Complex wavelet coefficients were converted to power by taking the square of the absolute value of each coefficient. Wavelet power is related to the temperature variance at each time and frequency location and is therefore presented in units of $^{\circ}C^2$ period^{-1}. The wavelet energy density was computed by taking the area for eight overlapping 6 h ranges staggered by 3 h,

involving periods from 1 to 28 h for the wavelet representation of each signal (range 1: from 1 to 7 h, range 2: from 4 to 10 h,... and range 8: from 22 to 28 h), and this value was then normalized by dividing by the total area from 1 to 28 h.

2.2.2. Circadian rhythm analysis. We computed the auto-correlation coefficient using a lag-time of 24 h for each signal (i.e. for patch temperature and actigraphy) after normalizing the signal to unit variance and subtracting its mean. This auto-correlation value has previously been termed r24 for the circadian rhythm analysis of the rest–activity cycle [18,19]. In accordance with the previously reported r24 analysis, the ZCM actigraphy signal was used for r24 analysis [18,19]. For all other actigraphy data analysis, PIM was used.

A fast Fourier transform (FFT), with a frequency resolution of 2.03×10^{-6} Hz, was computed for each temperature and rest–activity dataset after subtraction of the mean. If the maximum FFT magnitude existed at a period within a predefined circadian range (18.01–30 h), we considered the dataset had a 'dominant' circadian component.

We fit a sine wave with a period of 24 h to each temperature patch and actigraphy PIM dataset using a nonlinear least-squares approach with the Matlab Curve Fitting Toolbox to determine the 24 h amplitude and phase within 95% confidence limits for each signal. Phase information was used to determine the peak time for each signal.

Correlation coefficients between pairs of skin surface patches were computed for each subject. In addition, correlation coefficients were computed between the ambient temperature and each skin surface patch after skin temperature signals were low-pass filtered to one-half the ambient temperature sampling rate and then downsampled to the sampling rate of ambient temperature.

2.2.3. Statistical analyses. Statistics were computed using the Matlab Statistics Toolbox. Statistical significance was set as $p < 0.05$. Results are displayed as mean $\pm$ s.d. For testing proportion differences between groups, the Pearson χ^2-test was used. Mean temperatures and 24 h amplitudes as well as normalized wavelets were compared among groups using analysis of variance with a Tukey post hoc test or a paired *t*-test whenever appropriate.

3. RESULTS

Out of 55 skin surface thermal patches placed on subjects, 41 patches (75%) showed less than 20 per cent data loss and were used for subsequent analysis.

3.1. Skin temperature as a biomarker of chronotherapy

Fluctuations in skin temperature occurred throughout monitoring, but beyond the 24 h rhythm there was no trend in skin temperature measured for control subjects. Figure 3*a* shows an example of a control subject's skin temperature signal throughout the monitoring period where the mean 24 h temperature for all patches on this subject had a slight decrease of 0.14 ± 0.09°C each day. By contrast, in PAT 3, the skin temperature signal increased by 0.43 ± 0.04°C each day (figure 3*b*), throughout the administration of chronochemotherapy with chronoIFLO4 (figure 3*e*). Actigraphy measurements also revealed rhythm disruption throughout treatment delivery (figure 3*d*) while the rest–activity pattern remained stable in the control subject (figure 3*c*).

To identify ultradian rhythms in skin temperature, we used wavelet analysis to generate a time–frequency spectrum for each temperature signal. This allowed us to visualize the dynamics in skin temperature rhythms. An example of ultradian rhythm for skin temperature is the approximately 2 h rhythm that occurred each night for a control subject's spectra (figure 4*a*,*c*). This rhythm was less prominent on the chest compared with back locations (figure 4*a*,*c*).

Variations in ultradian skin temperature rhythms occurred during chronotherapy as shown for PAT 3. Thus, a 24 h rhythm was displayed across the full monitoring period for the example spectrum from a patch with a chest location. Ultradian rhythms with shorter periods also developed on this chest skin patch throughout treatment (figure 4*b*), illustrating changes in skin temperature dynamics at this location throughout the monitoring period. No such temporal modifications were obvious for a patch located on the back of the same subject (figure 4*d*).

All controls and patients had a peak time-averaged wavelet power occur within the circadian region of 18–28 h, except for one control subject, whose peak occurred at approximately 12 h (figure 5*a*,*b*). A smaller intensity peak at the first harmonic of the circadian rhythm, or a period of approximately 12 h, was recognized for controls, but not the patients.

The majority of normalized wavelet power occurred in the longer period ranges (6, 7 and 8) that overlap the circadian region (figure 6). For controls, ranges 4–8 all hold between 24 and 30 per cent of the total wavelet power followed by 19.6, 14.5 and 9.8 per cent for ranges 3, 2 and 1, respectively. The patient groups had higher normalized power in the circadian ranges 7 and 8 than the controls and lower normalized power in the shorter period ranges 1 through 4, showing an increase in ultradian rhythms for the controls compared with patients (figure 6).

3.2. Characteristics of circadian rhythms in skin temperature and activity

3.2.1. Regularity of circadian rhythm (r24 analysis). r24 correlations for ZCM actigraphy signals were on average lower for the patients than for the controls (0.18 ± 0.15 versus 0.45 ± 0.09), with both patients on chronotherapy having the lowest scores (0.07 and 0.08), indicating poor reproducibility of 24 h changes from one day to the next. The patient on the standard oral treatment regimen during monitoring had the next lowest r24 actigraphy (0.20). All controls and the patient without treatment had r24 actigraphy ranging from 0.3 to 0.6.

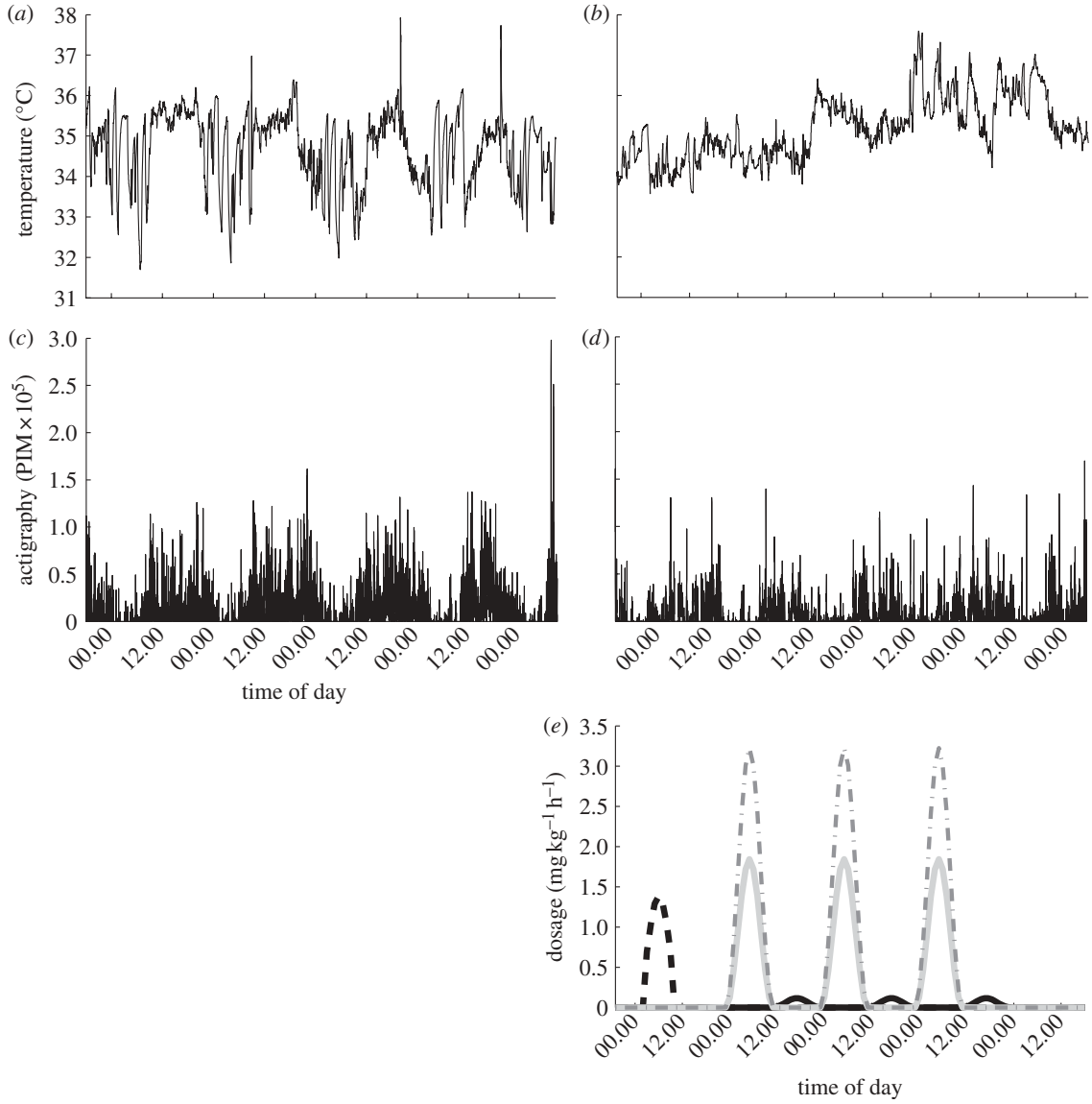

Figure 3. Representative data from (*a*,*c*) a control subject and (*b*,*d*) a cancer patient receiving (*e*) intensive chronotherapy with four anti-cancer drugs (chronoIFLO4). Repeatable patterns in the skin temperature from the control acquired from a warm location on the back (*a*) contrast with the steadily increasing (but with seemingly random changes) skin temperature from a warm location on the chest side of the patient (*b*) during treatment. Actigraphy patterns (PIM actigraphy data shown) for the control (*c*) show a consistent rest–activity cycle. Patient activity patterns (*d*) show sporadic activity, with less rest–awake periodicity compared with the control. The timed ChronoIFLO4 infusion schedule for the patient is shown in (*e*). (*e*) Dashed black line, CPT; solid black line, OHP; solid grey line, LV; dotted–dashed grey line, 5-FU.

r24 skin temperature values displayed large inter-subject variability. Figure 7 shows r24 skin temperature values for each patch analysed versus the r24 actigraphy in the same subject. The spread in r24 skin temperature was computed for each subject as the difference between the maximum and minimum r24 skin temperature values. The median spread of r24 skin temperature for all subjects was 0.39 (range from 0.18 to 0.57).

3.2.2. Circadian rhythms in skin temperature. The ability to identify a dominant circadian component by using skin surface temperature patches and PIM actigraphy measurements is illustrated in a control for FFT analysis (figure 8*a*,*b*) and 24 h curve fitting (figure 8*c*). Twenty-three out of the 41 skin temperature patches analysed (57%) had their maximum FFT amplitude occur within the circadian domain. Patches on the left side of the body were more likely to detect the dominant circadian component than patches on the right side ($p < 0.05$), while no difference was found for chest versus back locations or for IR-defined 'warm' or 'cool' locations (figure 9*a*). Actigraphy data from all subjects had maximum FFT amplitudes within the circadian domain. This was also the case for ambient temperature for all the subjects, except a patient whose study took place within the hospital setting.

3.2.3. Impact of patch location on circadian temperature amplitude. Twenty-four hour amplitudes from the curve-fitting procedure for each skin temperature signal with a dominant circadian component were averaged together within their respective groups (figure 9*b*).

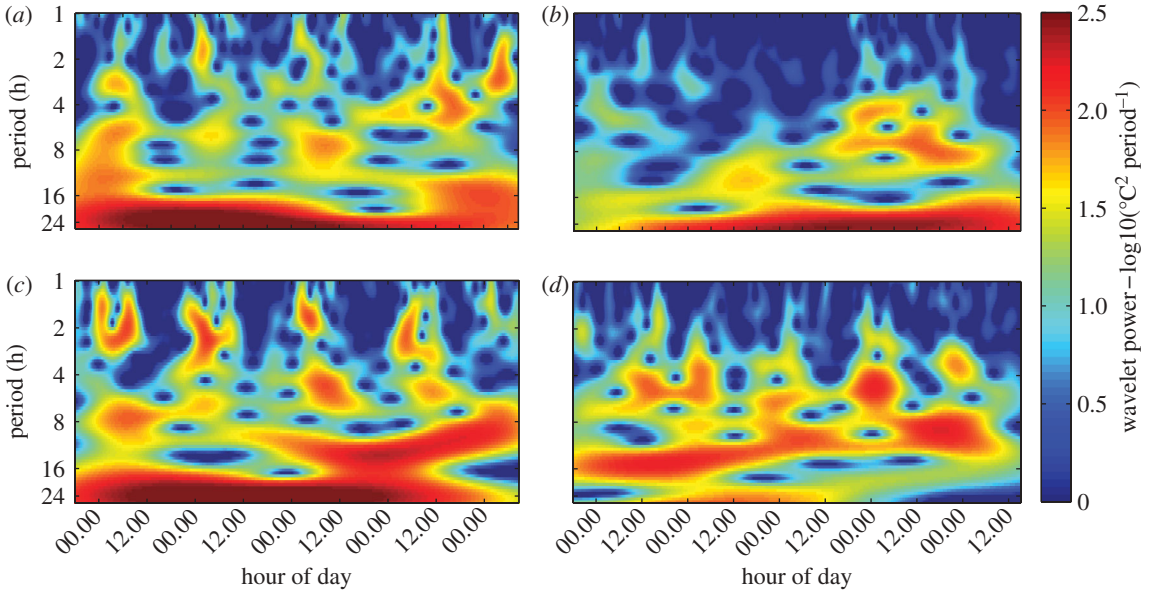

Figure 4. Skin temperature wavelet spectra. Rhythms in skin temperature of less than 24 h are shown in the time–frequency spectra for a thermal patch placed on a chest warm location for (*a*) a control and (*b*) a cancer patient. Time–frequency spectra for a back warm location for a control and a cancer patient are shown in (*c*,*d*), respectively. Besides the 24 h rhythms present in (*a*–*c*), significant power at ultradian rhythms can be seen on all the spectra, with dynamic changes. For instance, the patch shown in (*b*) for PAT 3 had maximum wavelet power (in periods of less than 16 h) of 20.13°C^2 period^{-1}, 48.52°C^2 period^{-1}, 53.06°C^2 period^{-1} and 87.54°C^2 period^{-1} for the first four 24 h monitoring periods, respectively.

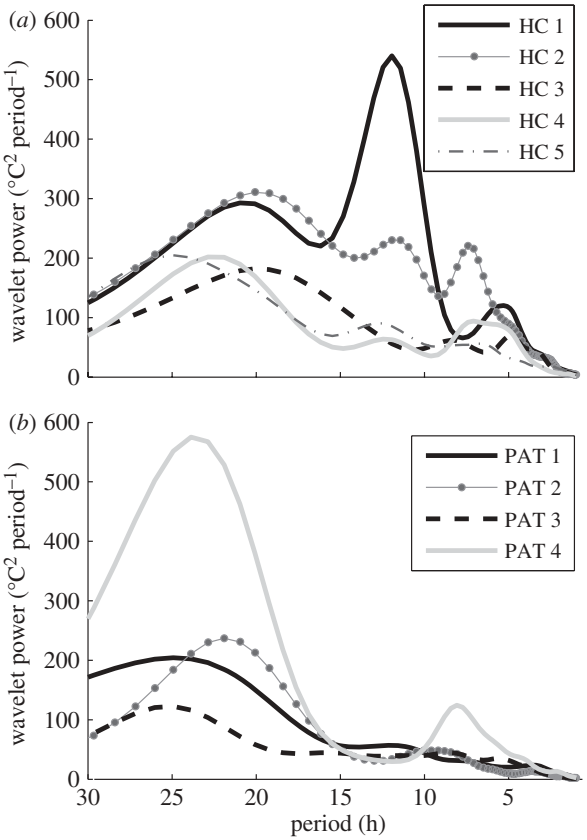

Figure 5. Differences between control and patient time-averaged wavelet spectra. Time-averaged wavelet spectra averaged for all patches for each subject for (*a*) healthy controls and (*b*) patients for periods ranging from 1 to 30 h. The only control subject not to have an approximately 24 h dominant period, HC 1, suffered from a chronic infection during monitoring, which may be responsible for the 12 h dominant period seen in (*a*).

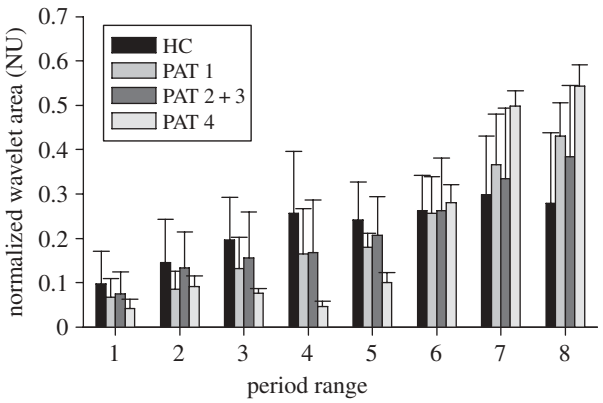

Figure 6. Ultradian and circadian frequency content from wavelet analysis. Area of normalized wavelet power (in normalized units) for eight overlapping period ranges from 1 to 28 h (range 1: from 1 to 7 h, range 2: from 4 to 10 h, . . . , range 8: from 22 to 28 h). All patches from healthy controls are averaged together, while the patches in cancer patients are split based on no or oral treatment or intensive intravenous chronochemotherapy.

Significant differences in the 24 h amplitude existed between IR-defined warm (0.50 ± 0.23°C) and cool (0.91 ± 0.26°C) groups ($p < 0.05$). Patches located in the middle had a higher mean 24 h amplitude than those on the right or the left side of the body ($p < 0.05$). No difference in circadian amplitude was found between the control and patient groups, nor between chest and back locations. Thus, the initial temperature value appeared to be the strongest determinant in the skin temperature circadian amplitude.

3.2.4. Circadian timing in temperature and activity rhythms. Controls had an average peak time in activity

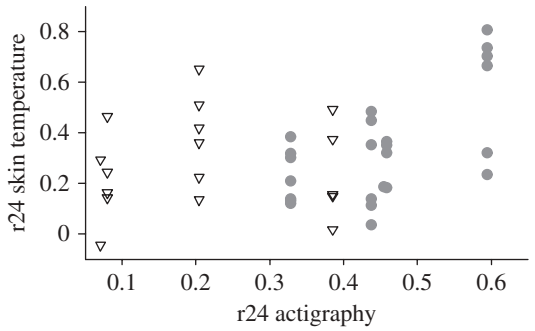

Figure 7. Relations between skin temperature and activity patterns: autocorrelation coefficients. r24 skin temperature versus r24 actigraphy. r24 value from thermal patches for each subject versus the subject's r24 value obtained from actigraphy (ZCM). Closed grey circles represent controls, and open triangles represent patients.

at 14.27 h ($\pm$2.5 h). The peak times in activity occurred at 13.48 and 14.45 h in both outpatients, PAT 1 who was not on treatment and PAT 4 who was receiving oral medications. Conversely, a phase advance in activity was apparent for both hospitalized patients on chronoIFLO4, with a maximum occurring at 11.46 h for PAT 2 and PAT 3 (figure 10).

Skin temperature peak times varied throughout the day across subjects. The median daily peak time in the temperature time series of each subject was 21.52 h ($\pm$5.4 h) in controls and 23.39 h ($\pm$2.2 h) in cancer patients. The median difference between the latest and the earliest peak times of the averaged 24 h temperature pattern was similar between control subjects and cancer patients (4.85 and 4.80 h, respectively).

3.3. Thermal characteristics of warm and cool skin areas

Patches with a higher initial mean temperature ($33.31 \pm 0.76^{\circ}$C) were designated as warm, and those with a lower mean temperature ($32.18 \pm 0.81^{\circ}$C) ($p = 0.001$) were designated as cool. The temperature of the warm and cool patches irrespective of location tended to converge over time, with average temperatures being, respectively, $34.62 \pm 0.85^{\circ}$C and $34.16 \pm 1.06^{\circ}$C ($p = 0.12$). However, qualification of the average temperature for chest or back locations revealed higher values for IR warm patches compared with IR cool patches ($p < 0.001$). The mean temperature did not significantly differ between controls and patients ($p = 0.06$), between chest and back ($p = 0.19$) or among right, middle and left locations ($p = 0.95$).

4. DISCUSSION

Continuously monitoring individual physiological rhythms during chronotherapy is useful not only for determining the circadian phase but also for identifying circadian disruption, either pre-existing or induced by anti-cancer treatments. Both kinds of information regarding the dynamics of the CTS could indeed be critical for the fine tuning of chronotherapeutic delivery in individual cancer patients, so as to deliver drugs both at their optimal internal timing and proper dose levels. Here, skin surface temperature was monitored for several days in five control subjects and four patients using VitalSense thermal patches. This system was susceptible to data loss during wireless transmission, possibly owing to the location of the monitor outside of the 2 m reception range from activated patches or interference from nearby electronics. We used a cubic spline procedure to fill in lost data points, a procedure that is not expected to impact the current range of interest for periods longer than 1 h. In so doing, 75 per cent of the patches provided relevant time series.

While circadian and ultradian patterns in skin surface temperature were rather stable in individual control subjects, this was not the case for both patients with advanced colorectal cancer receiving a standard intensive four-drug chronochemotherapy regimen. The modifications in the rhythmic organization of skin surface temperature could result from systemic inflammation, as well as from altered cardiovascular or metabolic processes related to the cytotoxic effects of the anti-cancer drugs.

Ultradian rhythms in skin temperature may be related to cycles in metabolic heat production, changes in skin blood flow, ambient temperature or any combination of these factors. Therefore, monitoring skin temperature rhythms with ultradian components may give us information about the current state of multiple cardiovascular and/or metabolic processes. Wavelet analysis revealed the existence of many ultradian rhythms whose prominence varied along the circadian time scale and along the course of treatment administration in cancer patients. This was supported by the occurrence of significant wavelet power throughout the 1–18 h ranges. Such ultradian components appeared to be more prominent in the controls, rather than in the cancer patients, suggesting that rhythm disruption could further extend to the ultradian domain in cancer patients. The single control not to show a dominant time-averaged wavelet peak in the circadian region, but instead at approximately 12 h, experienced an infectious sinusitis and menstruation phase onset during monitoring. These two processes are known to influence body temperature regulation.

The current study showed that repeatability of circadian rhythms in skin temperature over 24 h (as determined by r24 analysis) had a large variability within subjects, dependent upon the location of skin temperature patches. This illustrated the clinically meaningful impact of measurement location for skin temperature-based CTS assessment. This variability appeared independent of how prominent the rest–activity cycle was. Both inpatients monitored during chronomodulated cancer chemotherapy displayed the lowest r24 values for the rest–activity rhythm, possibly as a result of the systemic toxicity of anti-cancer drugs. Furthermore, it has been shown that even short-lasting anaesthesia can induce circadian disruption in otherwise healthy subjects [37], pinpointing the sensitivity of the CTS to external pharmacological manipulations. Indeed, the patient not on treatment was undergoing a typical daily routine and had a normal rest–activity

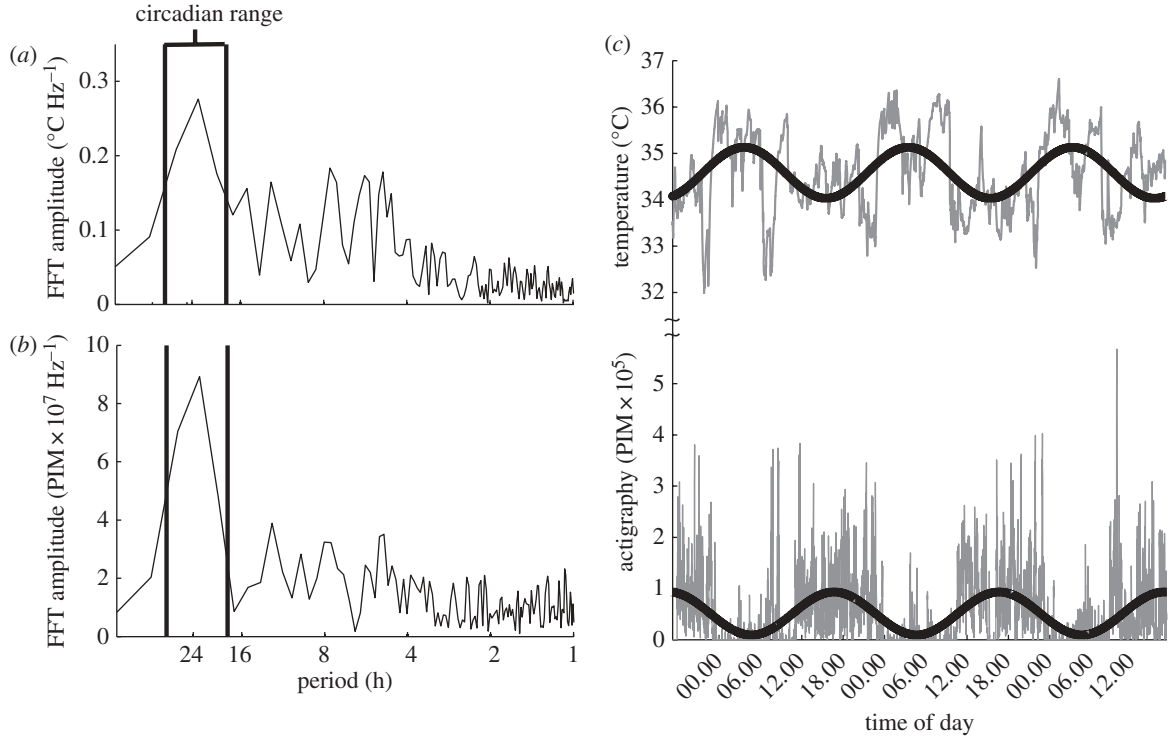

Figure 8. Relations between skin temperature and activity patterns: fast Fourier transforms. Representative FFTs and 24 h curve fitting. Frequency content from periods of 1–40 h for one skin temperature patch (*a*) and the corresponding actigraphy data (*b*) for the same subject both show dominant circadian rhythms. Vertical lines in (*a*,*b*) represent the pre-set circadian range from periods of 18–30 h. Raw thermal patch dataset (thin grey line) with 24 h sine fit (top thick black line) is shown at the top of (*c*) for the same signal with frequency spectrum shown in (*a*). The actigraphy signal (thin grey line) for the FFT in (*b*) is shown below the skin temperature signal, again with a 24 h sine fit (bottom thick black line).

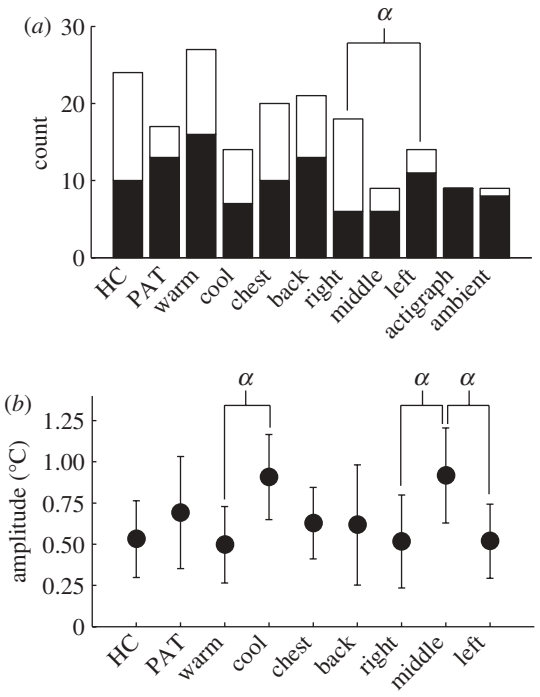

Figure 9. Detection of circadian patterns in skin surface temperature time series. The total number of patches that had a dominant circadian component for each group is shown out of the total number of patches for that group in (*a*). Mean amplitude for all skin temperature signals with a dominant circadian component, with error bars representing s.d., from the 24 h curve-fitting procedure is shown for each skin temperature group in (*b*). α denotes significance between marked groups with $p < 0.05$.

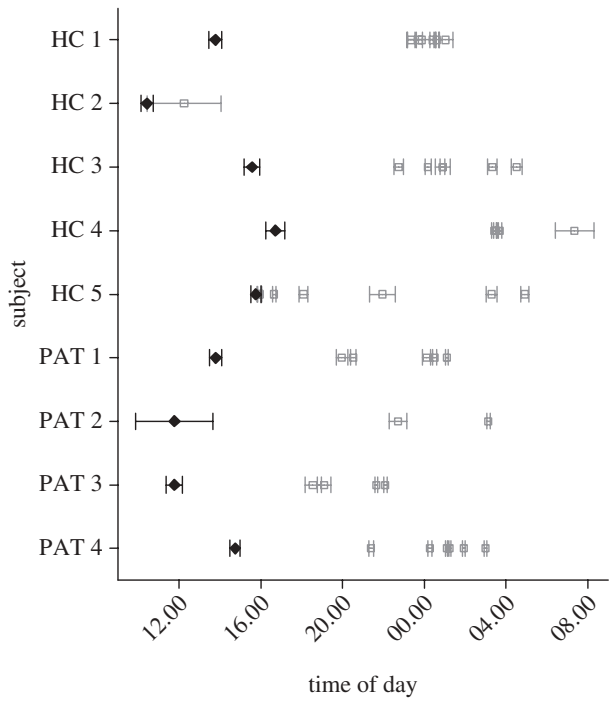

Figure 10. Relations between circadian phases of skin surface temperature and rest–activity. Twenty-four hour peak times for skin temperature and actigraphy data. Time of day of peak 24 h skin temperature (open grey squares) and actigraphy (filled black diamonds) by subject from 24 h curve fitting with 95% confidence limits.

cycle, while the oral medication patient had a slightly disrupted rest–activity cycle.

The high values in activity were similar in controls and in both outpatients receiving no chemotherapy or oral treatment. In contrast, both intensively treated patients on chronoIFLO4 displayed an approximately 3 h phase advance of their circadian rest–activity rhythm compared with both outpatients and the control subjects. Such phase advance could relate to the hospital routine, to patient chronotype, an issue not explored in this study, to advanced cancer and/or to chemotherapy toxicity. The circadian phases varied by up to 13 h between patches within a single individual (median of 4.8 h). Thus, measurement of the circadian rhythm at two locations on a single subject may produce two different phases, which may be clinically significant depending on the applications.

Multiple circadian clocks existing in different peripheral tissues with various periods may explain the inter-subject variability that we saw in the circadian rhythms of skin temperature [38,39]. The rest–activity cycle is controlled by the SCN, which is the main circadian oscillator, but peripheral clocks can affect a local tissue region to a greater extent [40,41]. Adipose tissue has been shown to have functional molecular circadian clocks that temporally modulate metabolism, and these could lead to local changes in the circadian rhythm of temperature across the surface of the body [42]. It has also been shown that a change in temperature itself plays an important role in regulating peripheral circadian clocks [27], so it may be that local temperature oscillations are important for fine adjustments in regional peripheral clocks in different tissues.

Previous studies have not taken into account the effect of possible local spatial variations in skin temperature on the circadian component of skin temperature [29,43], but this would only be appropriate if skin temperature were homogeneous across a given surface of the body. In the current study, IR imaging confirmed the heterogeneous pattern of skin temperatures measured at a single circadian time. Furthermore, this is the first time that differences in the circadian rhythm of skin temperature are shown between IR-defined warm and cool locations on the skin of the chest or upper back, with a near doubling of the circadian amplitude for the cool 'patches' as compared with the warm ones. Thus, if the goal is to monitor the circadian rhythm and phase over multiple days, then cool locations may be the better choice because the greater circadian temperature variance is a signature of a more prominent circadian rhythm. In addition, multiple locations should be measured to ensure that a location with a dominant circadian rhythm is being captured.

5. CONCLUSIONS

Superficial skin temperature monitoring on the upper torso as a method to determine the circadian phase and to identify disruption of biological rhythms has been investigated. We showed that circadian amplitude and phase in skin temperature vary across measurement sites for individual subjects, and specifically that locations identified as cool by the use of IR imaging had a larger 24 h amplitude than those identified as warm, pointing to the need for monitoring at multiple sites for accurate determination of the circadian phase. Additionally, in our limited sample size, we found that intensive standardized chronochemotherapy [44] may disrupt both circadian and ultradian rhythms. Recording of skin temperature at different locations might be useful for more precise identification of the individual phase of the CTS of patients and for dynamically tracking biological rhythms to optimize cancer chronotherapeutics. In future studies, temperature monitoring for personalized chronotherapeutics should be performed prior to and during chronotherapy to determine the CTS phase accurately, locate treatment-induced circadian disruption, track specific ultradian rhythms and adjust treatment doses and timing accordingly.

This research was supported, in part, by the European Commission through the Network of Excellence BIOSIM (Biosimulation: a new tool for drug development; contract no. LSHBCT-2004-005137), the Association pour la Recherche sur le Temps Biologique et la Chronothérapie (ARTBC International), Hôpital Paul Brousse, Villejuif (France) and the Intramural Research Programme of the National Institute of Biomedical Imaging and Bioengineering, National Institutes of Health (USA). The authors thank the subjects who participated in the study, Dr G. Kato, Dr H. Ackerman and A. Dementyev for insightful discussions and J. Bretes, FLIR Systems ATS France for the loan of infrared equipment and assistance for this study.

REFERENCES

1 Panda, S., Hogenesch, J. B. & Kay, S. A. 2002 Circadian rhythms from flies to human. *Nature* **417**, 329–335. (doi:10.1038/417329a)
2 Reppert, S. M. & Weaver, D. R. 2002 Coordination of circadian timing in mammals. *Nature* **418**, 935–941. (doi:10.1038/nature00965)
3 Ashall, L. *et al.* 2009 Pulsatile stimulation determines timing and specificity of NF-κB-dependent transcription. *Science* **324**, 242–246. (doi:10.1126/science.1164860)
4 Dibner, C., Schibler, U. & Albrecht, U. 2010 The mammalian circadian timing system: organization and coordination of central and peripheral clocks. *Annu. Rev. Physiol.* **72**, 517–549. (doi:10.1146/annurev-physiol-021909-135821)
5 Lévi, F., Okyar, A., Dulong, S., Innominato, P. F. & Clairambault, J. 2010 Circadian timing in cancer treatments. *Annu. Rev. Pharmacol. Toxicol.* **50**, 377–421. (doi:10.1146/annurev.pharmtox.48.113006.094626)
6 Takahashi, J. S., Hong, H.-K., Ko, C. H. & Mcdearmon, E. L. 2008 The genetics of mammalian circadian order and disorder: implications for physiology and disease. *Nat. Rev. Genet.* **9**, 764–775. (doi:10.1038/nrg2430)
7 Lévi, F., Focan, C., Karaboué, A., De La Valette, V., Focan-Henrard, D., Baron, B., Kreutz, F. & Giacchetti, S. 2007 Implications of circadian clocks for the rhythmic delivery of cancer therapeutics. *Adv. Drug Deliv. Rev.* **59**, 1015–1035. (doi:10.1016/j.addr.2006.11.001)
8 Altinok, A., Lévi, F. & Goldbeter, A. 2007 A cell cycle automaton model for probing circadian patterns of

anticancer drug delivery. *Adv. Drug Deliv. Rev.* **59**, 1036–1053. (doi:10.1016/j.addr.2006.09.022)
9 Altinok, A., Lévi, F. & Goldbeter, A. 2009 Identifying mechanisms of chronotolerance and chronoefficacy for the anticancer drugs 5-fluorouracil and oxaliplatin by computational modeling. *Eur. J. Pharm. Sci.* **36**, 20–38. (doi:10.1016/j.ejps.2008.10.024)
10 Bernard, S., Čajavec Bernard, B., Lévi, F. & Herzel, H. 2010 Tumor Growth rate determines the timing of optimal chronomodulated treatment schedules. *PLoS Comput. Biol.* **6**, e1000712. (doi:10.1371/journal.pcbi.1000712)
11 Lévi, F., Altinok, A. & Goldbeter, A. 2010 *Circadian rhythms and chronotherapeutics*, ch. 15 (eds F. Marcus & A. Cesario). New York, NY: Springer Verlag.
12 Lévi, F., Zidani, R. & Misset, L. 1997 Randomised multicentre trial of chronotherapy with oxaliplatin, fluorouracil, and folinic acid in metastatic colorectal cancer. *Lancet* **350**, 681–686. (doi:10.1016/S0140-6736(97)03358-8)
13 Giacchetti, S. *et al.* 2006 Phase III trial comparing 4-day chronomodulated therapy versus 2-day conventional delivery of fluorouracil, leucovorin, and oxaliplatin as first-line chemotherapy of metastatic colorectal cancer: The European Organisation for Research and Treatment of Cancer Chronotherapy Group. *J. Clin. Oncol.* **24**, 3562–3569. (doi:10.1200/jco.2006.06.1440)
14 Giacchetti, S. *et al.* In preparation. Relevance of gender for optimal efficacy of chronomodulated versus conventional delivery of 5-fluorouracil-leucovorin and oxaliplatin as first line treatment for metastatic colorectal cancers in first meta-analysis of three international randomized trials using individual patient data.
15 Filipski, E., Innominato, P. F., Wu, M., Li, X.-M., Iacobelli, S., Xian, L.-J. & Lévi, F. 2005 Effects of light and food schedules on liver and tumor molecular clocks in mice. *J. Natl Cancer Inst.* **97**, 507–517. (doi:10.1093/jnci/dji083)
16 Filipski, E., King, V. M., Li, X., Granda, T. G., Mormont, M.-C., Liu, X., Claustrat, B., Hastings, M. H. & Lévi, F. 2002 Host circadian clock as a control point in tumor progression. *J. Natl Cancer Inst.* **94**, 690–697. (doi:10.1093/jnci/94.9.690)
17 Lee, S., Donehower, L. A., Herron, A. J., Moore, D. D. & Fu, L. 2010 Disrupting circadian homeostasis of sympathetic signaling promotes tumor development in mice. *PLoS ONE* **5**, e10995. (doi:10.1371/journal.pone.0010995)
18 Innominato, P. F. *et al.* 2009 Circadian rhythm in rest and activity: a biological correlate of quality of life and a predictor of survival in patients with metastatic colorectal cancer. *Cancer Res.* **69**, 4700–4707. (doi:10.1158/0008-5472.can-08-4747)
19 Mormont, M.-C. *et al.* 2000 Marked 24-h rest/activity rhythms are associated with better quality of life, better response, and longer survival in patients with metastatic colorectal cancer and good performance status. *Clin. Cancer Res.* **6**, 3038–3045.
20 Sephton, S. E., Sapolsky, R. M., Kraemer, H. C. & Spiegel, D. 2000 Diurnal cortisol rhythm as a predictor of breast cancer survival. *J. Natl Cancer Inst.* **92**, 994–1000. (doi:10.1093/jnci/92.12.994)
21 Iurisci, I., Filipski, E., Reinhardt, J., Bach, S., Gianella-Borradori, A., Iacobelli, S., Meijer, L. & Lévi, F. 2006 Improved tumor control through circadian clock induction by seliciclib, a cyclin-dependent kinase inhibitor. *Cancer Res.* **66**, 10720–10728. (doi:10.1158/0008-5472.can-06-2086)
22 Li, X.-M., Delaunay, F., Dulong, S., Claustrat, B., Zampera, S., Fujii, Y., Teboul, M., Beau, J. & Lévi, F. 2010 Cancer inhibition through circadian reprogramming of tumor transcriptome with meal timing. *Cancer Res.* **70**, 3351–3360. (doi:10.1158/0008-5472.can-09-4235)
23 Innominato, P. F., Mormont, M.-C., Rich, T. A., Waterhouse, J., Lévi, F. A. & Bjarnason, G. A. 2009 Circadian disruption, fatigue, and anorexia clustering in advanced cancer patients: implications for innovative therapeutic approaches. *Integr. Cancer Ther.* **8**, 361–370. (doi:10.1177/1534735409355293)
24 Czeisler, C. A. *et al.* 1999 Stability, precision, and near-24-hour period of the human circadian pacemaker. *Science* **284**, 2177–2181. (doi:10.1126/science.284.5423.2177)
25 Klerman, E. B., Gershengorn, H. B., Duffy, J. F. & Kronauer, R. E. 2002 Comparisons of the variability of three markers of the human circadian pacemaker. *J. Biol. Rhythm.* **17**, 181–193. (doi:10.1177/074873002129002474)
26 Moore-Ede, M. C., Czeisler, C. A. & Richardson, G. S. 1983 Circadian timekeeping in health and disease. *New Engl. J. Med.* **309**, 469–476. (doi:10.1056/NEJM198308253090806)
27 Brown, S. A., Zumbrunn, G., Fleury-Olela, F., Preitner, N. & Schibler, U. 2002 Rhythms of mammalian body temperature can sustain peripheral circadian clocks. *Curr. Biol.* **12**, 1574–1583. (doi:10.1016/S0960-9822(02)01145-4)
28 Krauchi, K. & Deboer, T. 2010 The interrelationship between sleep regulation and thermoregulation. *Front. Biosci.* **15**, 604–625. (doi:10.2741/3636)
29 Van Someren, E. J. W. 2006 Mechanisms and functions of coupling between sleep and temperature rhythms. *Prog. Brain Res.* **153**, 309–324. (doi:10.1016/S0079-6123(06)53018-3)
30 Gholam, D. *et al.* 2006 Chronomodulated irinotecan, oxaliplatin, and leucovorin-modulated 5-fluorouracil as ambulatory salvage therapy in patients with irinotecan- and oxaliplatin-resistant metastatic colorectal cancer. *Oncologist* **11**, 1072–1080. (doi:10.1634/theoncologist.11-10-1072)
31 Lévi, F. *et al.* 2010 Cetuximab and circadian chronomodulated chemotherapy as salvage treatment for metastatic colorectal cancer (mCRC): safety, efficacy and improved secondary surgical resectability. *Cancer Chemother. Pharmacol.* 1–10. (doi:10.1007/s00280-010-1327-8)
32 Blackwell, T., Redline, S., Ancoli-Israel, S., Schneider, J. L., Surovec, S., Johnson, N. L., Cauley, J. A. & Stone, K. L. 2008 Comparison of sleep parameters from actigraphy and polysomnography in older women: the SOF study. *Sleep* **31**, 283–291.
33 Jean-Louis, G., Kripke, D. F., Mason, W. J., Elliott, J. A. & Youngstedt, S. D. 2001 Sleep estimation from wrist movement quantified by different actigraphic modalities. *J. Neurosci. Methods* **105**, 185–191. (doi:10.1016/S0165-0270(00)00364-2)
34 Frick, P., Baliunas, S. L., Galyagin, D., Sokoloff, D. & Soon, W. 1997 Wavelet analysis of stellar chromospheric activity variations. *Astrophys. J.* **483**, 426. (doi:10.1086/304206)
35 Frick, P., Grossmann, A. & Tchamitchian, P. 1998 Wavelet analysis of signals with gaps. *J. Math. Phys.* **39**, 4091–4107. (doi:10.10631/1.532485)
36 Tankanag, A. & Chemeris, N. 2008 Application of the adaptive wavelet transform for analysis of blood flow oscillations in the human skin. *Phys. Med. Biol.* **53**, 5967. (doi:10.1088/0031-9155/53/21/005)
37 Dispersyn, G., Touitou, Y., Coste, O., Jouffroy, L., Lleu, J. C., Challet, E. & Pain, L. 2009 Desynchronization of daily rest–activity rhythm in the days following light propofol anesthesia for colonoscopy. *Clin. Pharmacol. Ther.* **85**, 51–55. (doi:10.1038/clpt.2008.179)

38 Brown, S. A. *et al.* 2005 The period length of fibroblast circadian gene expression varies widely among human individuals. *PLoS Biol.* **3**, e338. (doi:10.1371/journal.pbio.0030338)
39 Brown, S. A., Kunz, D., Dumas, A., Westermark, P. O., Vanselow, K., Tilmann-Wahnschaffe, A., Herzel, H. & Kramer, A. 2008 Molecular insights into human daily behavior. *Proc. Natl Acad. Sci. USA* **105**, 1602–1607. (doi:10.1073/pnas.0707772105)
40 Hastings, M. H., Reddy, A. B. & Maywood, E. S. 2003 A clockwork web: circadian timing in brain and periphery, in health and disease. *Nat. Rev. Neurosci.* **4**, 649–661. (doi:10.1038/nrn1177)
41 Stratmann, M. & Schibler, U. 2006 Properties, entrainment, and physiological functions of mammalian peripheral oscillators. *J. Biol. Rhythm.* **21**, 494–506. (doi:10.1177/0748730406293889)
42 Zvonic, S. *et al.* 2006 Characterization of peripheral circadian clocks in adipose tissues. *Diabetes* **55**, 962–970. (doi:10.2337/diabetes.55.04.06.db05-0873)
43 Van Someren, E. J. W. 2000 More than a marker: interaction between the circadian regulation of temperature and sleep, age-related changes, and treatment possibilities. *Chronobiol. Int. J. Biol. Med. Rhythm Res.* **17**, 313–354. (doi:10.1081/CBI-100101050)
44 Innominato, P. F., Lévi, F. A. & Bjarnason, G. A. 2010 Chronotherapy and the molecular clock: clinical implications in oncology. *Adv. Drug Deliv. Rev.* **62**, 979–1001. (doi:10.1016/j.addr.2010.06.002)